An investigation of plastic deformation behaviour of Nb-V microalloyed steel produced by powder metallurgy

D. Taştemür, S. Gündüz*

Karabük University, Technology Faculty, Karabük, Türkiye
Karabük University, Technology Faculty, Karabük, Türkiye
*Corresponding author: sgunduz@karabuk.edu.tr

(Received 26 December 2023; Accepted 28 October 2024)

Abstract

In this study, Nb-V microalloyed steel was produced and sintered at 1150 °C for 1 h followed by cooling in furnace. While one of the sintered samples was used in the sintered condition, the other one was cooled in air after homogenisation heat treatment at 1150 °C for 1 hour. The remaining samples were deformed at 20%, 40% and 60% in the temperature range 1150-930 °C and then cooled in air. Microstructure and precipitates formation of samples were investigated by optic microscope, scanning electron microscope and energy dispersive spectroscopy analyses. It was observed that samples showed smaller grain size, but higher volume fractions of ferrite under homogenised and 20%, 40% or 60% deformed conditions. This indicated that grain refinement and ferrite formation is accelerated with the deformation which affect the nucleation rate of ferrite. Also, the yield strength, hardness and density increased by the increase in deformation rate.

Keywords: Microalloyed steels; Powder metallurgy; Thermomechanical processing; Microstructure and mechanical properties

1. Introduction

The name “microalloyed steel” was first applied to low carbon steels containing Nb and/or V. Any attempt at a rational definition of microalloying based on the increase in strength produced by small additions would now include Al, V, Ti and of course Nb-treated steels. Such steels contain less than 0.1 wt.% of the alloying additions and yield strength increases of up to two times that of a plain carbon-manganese steel can be attained. It would appear that "microalloyed steels” as a name was reserved for the steels containing small amount of an alloying element which will produce grain refinement and/or precipitation hardening by the formation of stable carbides or nitrides [1, 2].

Thus, microalloyed steel will typically contain Nb, Ti or V and their specific effects may be influenced by other alloying additions such as Al or B. The effects of the microalloying elements are also strongly influenced by thermal and thermomechanical treatments [1-4]. The effective utilisation of Nb, Ti or V increase the mechanical properties achieved by thermomechanical processing in microalloyed steels and therefore it is important to understand the fundamental behaviour of the elements such as solubility, precipitation of carbide or nitride and retardation of austenitic recrystallisation [5-7]. The primary function of the microalloys is brought about through their carbonitrides, which can influence the properties of steel through various mechanisms such as grain refinement and precipitation strengthening [8].

Nb, Ti, and V are now widely used for their ability to increase the mechanical properties of steel. It is understood that these elements exert their powerful influence mainly through their behaviour during and subsequent to the hot deformation processing of austenite. The microalloying elements prevent the movement of grain boundaries, recrystallization boundaries and dislocations when they are present either as solute or as precipitates [2,9]. When microalloying elements are in solid solution in austenite, these elements can also increase hardenability, therefore leading to lower transformation temperatures. The suppression of both grain coarsening and recrystallization contributes to the control of the austenite microstructure, while this effect together with the hardenability effect act to control the final microstructure [9-11].

The minor addition of Nb to steel prevents the recrystallization of austenite and to achive finer microstructure. A similar effect is also seen in Ti added steels. However, it was observed that this effect is less marked in V added steels [5, 12]. V is widely used in microalloyed steel due to its higher solubility in the austenite compared to Nb and Ti [13]. V forms VCN at lower temperatures than Nb and Ti. If the austenitising temperature is high, the carbonitrides will dissolve and more free V will be in solid solution before cooling. This will increase the hardness of the steel. Likewise, if the composition of the precipitates is in such a ratio that they cannot dissolve at the austenitising temperature, less V will be in solution and lower hardenability will be obtained [14].

The production of microalloyed steels is carried out by casting, rolling and controlled cooling methods. However, the difficulty and cost of the production stages of microalloyed steels have led to produce these steels with powder metallurgy (PM) [15]. Therefore, microalloyed steel has been produced using the powder metallurgy in recent years. Powder metallurgy was developed as an alternative method to hot and cold pressing, traditional casting and machining methods. In this method, parts that are difficult to manufacture are produced in powder form with minimum tolerances and high strength compared to other production methods. In other words, the production of parts by pressing metal powders in accordance with the size and shape and sintering them in a protective gas atmosphere or under vacuum in the temperature range of 0.75-0.86Tm (Tm: melting temperature) is defined as powder metallurgy [16].

The high quality and rapid production of parts has made powder metallurgy to preferer over other classical methods. However, besides the advantages of the PM method, it also has some disadvantages [17]. The biggest disadvantage of powder metallurgy is the porous structure which cannot be completely eliminated and the density is lower than the materials produced by the conventional casting method [18]. Literature investigations indicated that the techniques and metallurgical basis for the processes involved have not previously been drawn together in a single work. The aim of this study is to minimize the porous structure of Nb-V microalloyed PM steel by thermomechanical processes and to improve mechanical properties by controlling density and precipitate formation simultaneously. These are the most important innovation and difference of this work.

2. Materials and methods

In the present work, a microalloyed steel in the composition of Fe-0.35C-0.1Nb-0.1V (wt.%) was produced by PM method. Fe, graphite, Nb and V powders of 45 μm, 10-20 μm, <45 μm, 45 μm were used with purities of 99,9%, 96,5%, 99,5% and 99,8%, respectively. It was observed that Fe powder is mostly irregular in shape and graphite powder is in flake shape.

Nb and V powders have an irregular shape and sharp-cornered geometry. SEM images of the powders are seen in Figure 1.

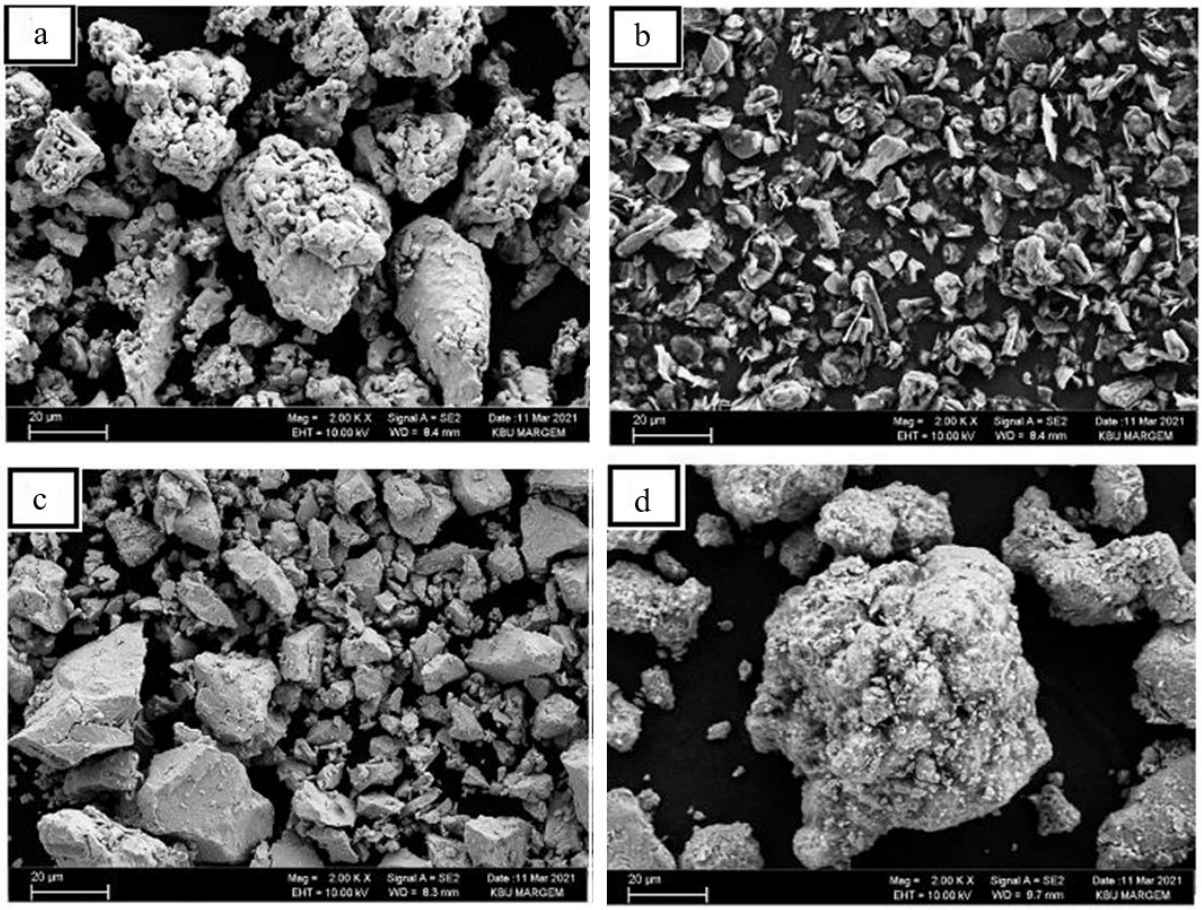

Figure 1. SEM images of (a) Fe, (b) Graphite, (c) Nb and (d) Ti powders.

A digital precision balance was used to weigh the powders at the required mass. Weighed powders were mixed in a turbula device for 3 hours. The mixed powders were pressed at 700 MPa in a hydraulic pressure with 96-ton capacity. 5 cylindrical samples in dimension of Ø32x29 mm were produced by cold pressing according to ASTM E9 standards. Pressed samples were sintered at 1150 °C for 1 h under argon atmosphere and then cooled to room temperature in the furnace. Figure 2 shows schematic presentation of sintering process.

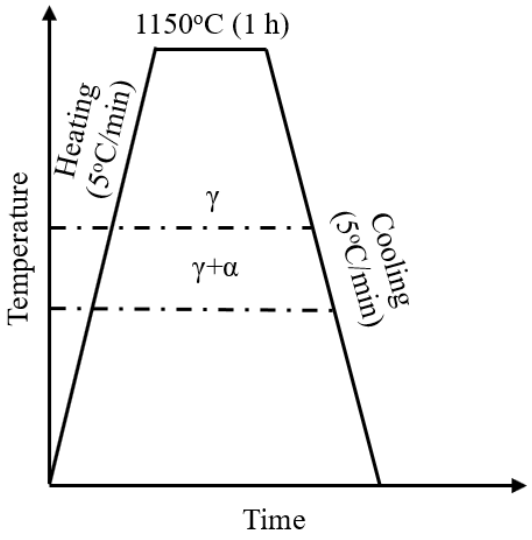

Figure 2. Schematic presentation of sintering process.

While one of the sintered samples was used in the sintered condition, the other one was cooled in air after homogenisation heat treatment at 1150 °C for 1 h. The remaining samples were deformed at 20%, 40% and 60% in the temperature range of 1150-930 °C at a strain rate of $2{,}8x10^{-1}$ s^{-1} and then cooled in air. Temperature measurements during deformation were carried out with a double laser heat meter. Figure 3 and 4 show the process steps used in the experimental study and the samples produced under different conditions respectively.

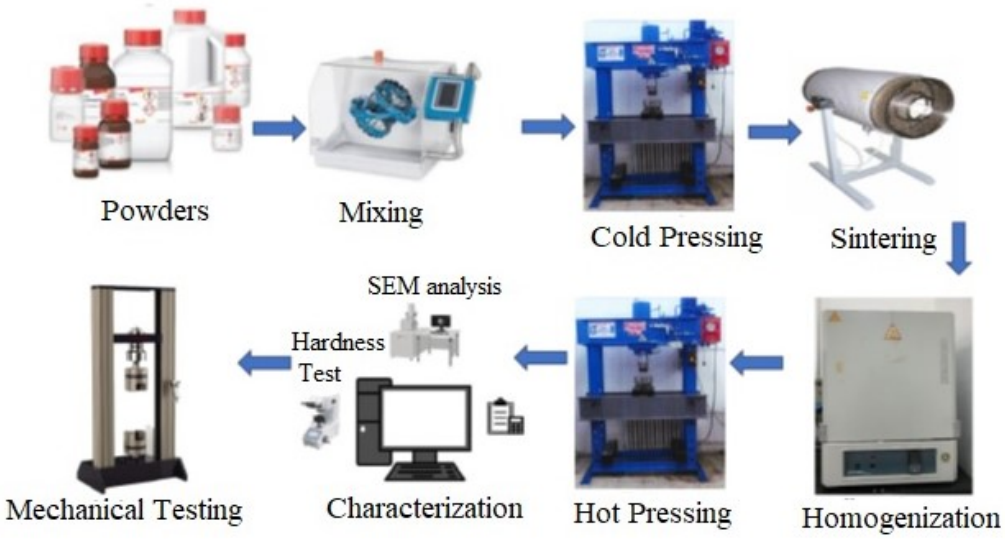

Figure 3. Process steps used in the experimental study.

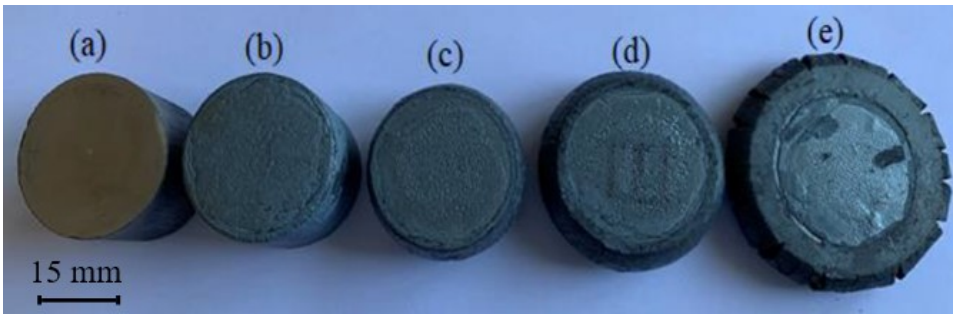

Figure 4. Produced samples a) sintered, b) homogenized, c) 20%, d) 40% and e) 60% deformed.

The chemical composition of produced Fe-0.35C-0.1Nb-0.1V (wt.%) samples was determined by spectral analysis method. Three different measurements were made on the produced sample and the average of these was accepted as chemical composition of steel. The results are given in Table 1. Spectral analysis results show that the planned chemical composition before production and obtained chemical composition after production are compatible with each other.

Table 1. Spectral analysis results of sintered Fe-0.35C-0.1Nb-0.1V (wt.%) steel.

Sintered	C (wt.%)	Nb (wt.%)	V (wt.%)	Fe (wt.%)
1	0.346	0.135	0.113	98.669
2	0.386	0.114	0.132	98.685
3	0.392	0.105	0.097	98.568
Average	0.375	0.118	0.114	98.61

The microstructure examinations of the sintered, homogenized, 20%, 40% and 60% deformed samples were carried out by optic microscope (OM) and scanning electron microscope (SEM). For metalographic examinations, samples were ground, polished and etched in 2% Nital solution to show the microstructure. Grain size and ferrite or pearlite volume fractions were measured by mean linear intercept and point count methods respectively. The sintered density were obtained through water displacement using Archimedes' principle. Compression tests were done at 1 mm/min crosshead speed using a 200 kN capacity BESMAK brand Electromechanical test machine at room temperature. Hardness measurements were done by applying a load of Hv0.5 (500 g). The average of 10 hardness measurements is used as the microhardness value.

3. Results and discussion

Figure 5 and Figure 6 reveal the OM and SEM microstructures of Fe-0.35C-0.1Nb-0.1V microalloyed PM steel under sintered, homogenised, 20%, 40% and 60% deformed conditions. It was observed that the structure consists of ferrite, pearlite and a porous structure. As is seen, the porous structure is evident in the sintered and homogenized sample and the porous structure and grain size decreases with increasing deformation rate. For example, the grain sizes of the sintered and homogenised samples are 23 μm and 19 μm respectively. It is clearly seen that the homogenised samples have smaller grains than the sintered samples. This is due to the fact that homogenised samples were cooled faster than sintered samples. At higher cooling rates such as air cooling, grain refinement occurs before the austenite-ferrite transformation [19]. Also, the grain sizes decreased to 18 μm, 16 μm and 14 μm when the

deformation rate increased to 20%, 40% and 60% respectively. Nb is an element that allows significant dissolution of NbCN at high temperatures. However, carbonitrides show low solubility at low temperatures of austenite. At these temperatures, undissolved carbonitride often acts as an effective grain refiner [20]. NbC precipitates, especially occured in the austenite region (900ºC-1300ºC), inhibit recrystallization and form small ferrite grains. Nb and V precipitate as carbides, nitrides or carbonitrides and increase the strength of steels through grain refinement, solid solution hardening and precipitation strengthening [6,21-23].

Precipitation strengthening is the most desired mechanism which is occurred by the formation of VC-like precipitates, especially in forging products. The type, size and distribution of precipitate particles are important for hardening. V is the most important element due to its high solubility in austenite [13]. The main function of V is precipitation hardening and carbon rich VCN is formed at temperatures below 700ºC. V precipitates with the size of less than 0.03 µm occur during or after transformation. VN can form in the austenite of medium carbon steels, especially when the amount of N is high, and can refine the structure similarly to NbC [2,24,25].

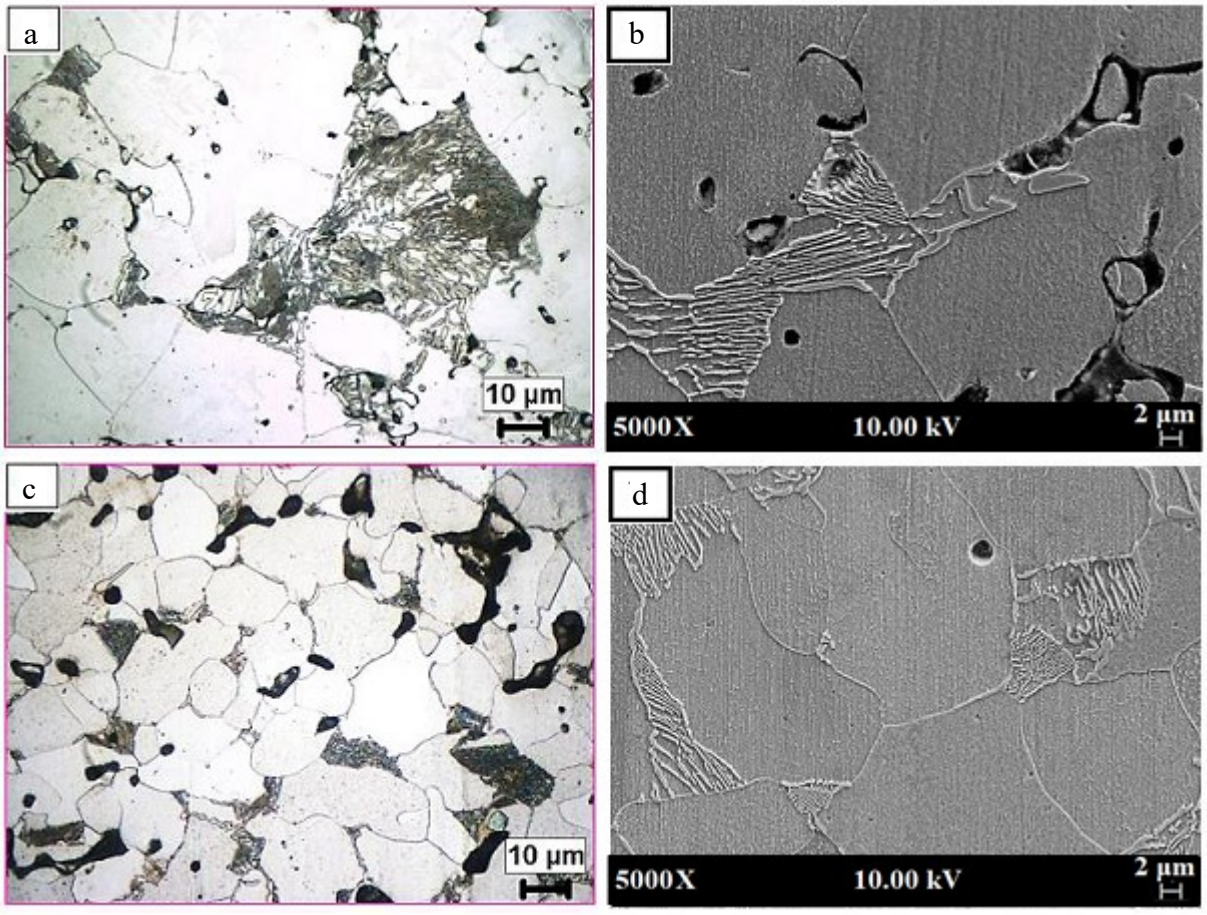

Figure 5. OM and SEM microstructure of the PM microalloyed steel at different magnifications; (a,b) sintered and (c,d) homogenised samples.

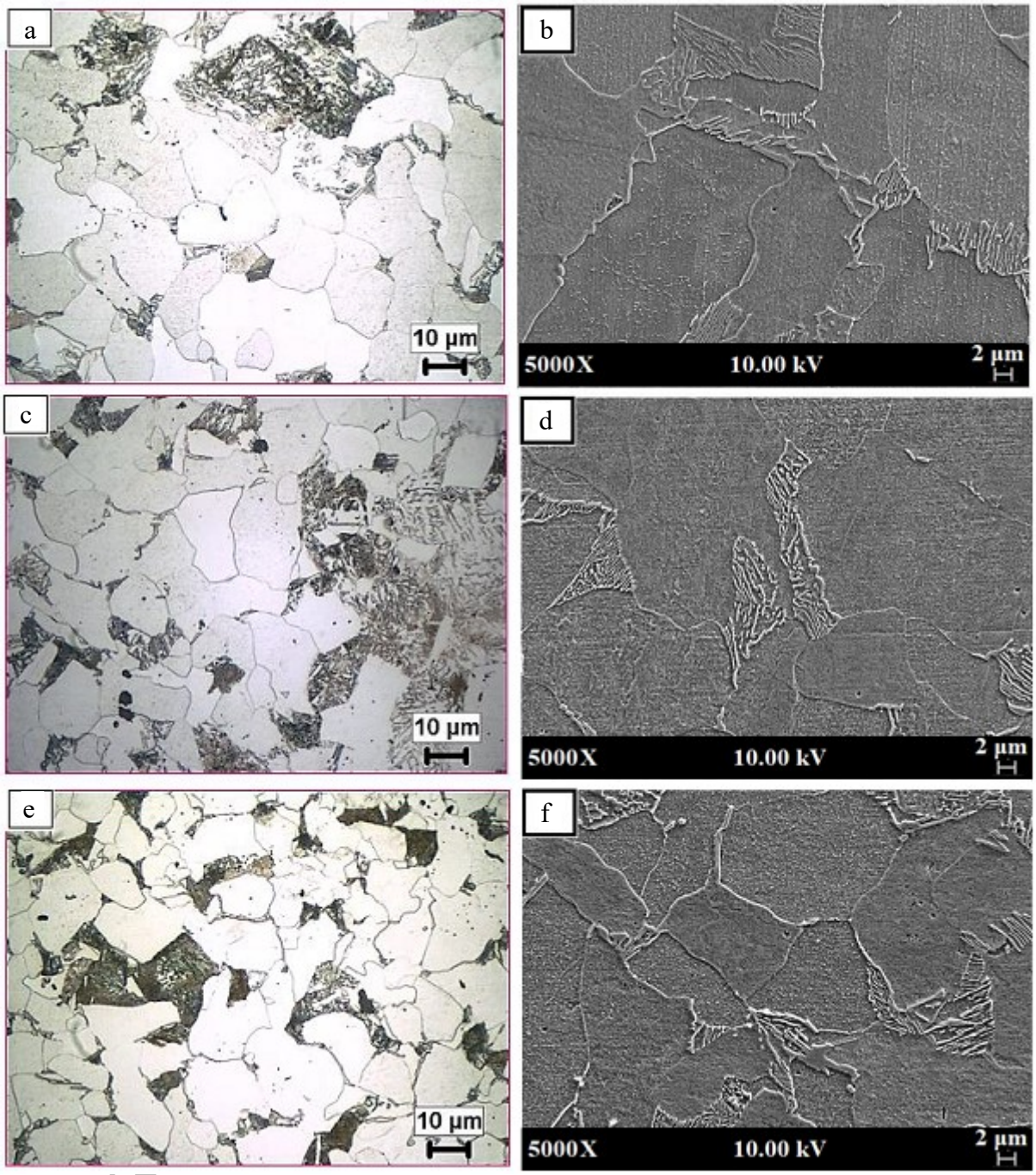

Figure 6. OM and SEM microstructure of the PM microalloyed steel at different magnifications; (a,b) 20%, (c,d) 40% and (e,f) 60% deformed samples.

Table 2 also gives density (%), porosity (%), pearlite (%), ferrite (%) and average grain size values of PM microalloyed steel samples under different conditions. As is seen in Table 2, the density (%) values of the sintered and homogenised sample are 90% and 89% respectively. When the samples deformed at 20%, 40% and 60%, a continuous increase in density to 96%, 97% and 98% was noticed respectively. Alloying generally decreases the density, but sintering temperatures, sintering times and deformation rate increase the density of PM alloys [26,27]. It was also observed from Table 2 that ferrite volume fraction of homogenised and deformed samples increased compared to the sintered samples. This is due to smaller grain

sizes in homogenised and deformed samples which accelerated nucleation rate of ferrite. Deformation also increases the nucleation rate by rising the amount of strained region at the austenite grain and grain boundaries [28,29]

Table 2. Density (%), pores (%), ferrite (%), pearlite (%) and grain size values of PM microalloyed steel.

PM steel	Density (%)	Pores (%)	Ferrite (%) ± σ (SD)	Pearlite (%) ± σ (SD)	Grain sizes (μm) ± σ (SD)
Sintered	90	9	77±0,48	23±0,87	23±0,73
Homogenised	89	10	80±0,44	20±0,89	19±0,61
20% deformed	96	3	84±0,40	16±0,91	18±0,55
40% deformed	97	2	85±0,39	15±0,92	16±0,49
60% deformed	98	1	87±0,36	13±0,93	14±0,43

Figure 7 reveal the line EDS results of sintered and 20% deformed samples. The line EDS analyses were carried out at the cross-section of the matrix and precipitate particles. EDS results, showing the concentration distribution of Fe, C, Nb and V along the line in Figure 7, indicated that niobium-rich (V-Nb)C precipitates are formed in the structure and these precipitates are located at the grain or grain boundaries. Among all microalloying elements, Nb is the strongest element to retard the recrystallization of austenite through the solute drag effect or deformation-induced precipitation. Inhibition of recrystallization leads to the formation of dislocations, deformation bands, twinning bands and subgrain structure which is well-known strong sites for nucleation and accelerate the precipitation process in the deformed microstructure [30].

In the traditional PM processes Mn is also used as alloying elements, because Mn influences the precipitation behaviour of microalloy carbonitrides in austenite during thermomechanical processing [31]. For example, the precipitation kinetics of Nb(CN) was investigated by Akben et.al [32] in the steel with Mn content between 0.5-1.6 wt.%. They found that increasing Mn content in Nb microalloyed steels delayed the dynamic precipitation of Nb(CN). They attributed the delay effect to the influence of Mn on the activity coefficients of the precipitating species, as a result of which the carbonitride solubility was increased [33]. Also, Grajcar et.al [34] investigated the effect of Mn on phase equilibrium and austenite decomposition in high strength steel. They found that the various Mn content influences the hardenability and hence the austenite decomposition during cooling. It should be pointed out that Mn concentration in microalloyed steel is important and it effects thermodynamics and kinetics of static strain-induced precipitates in microalloyed steels.

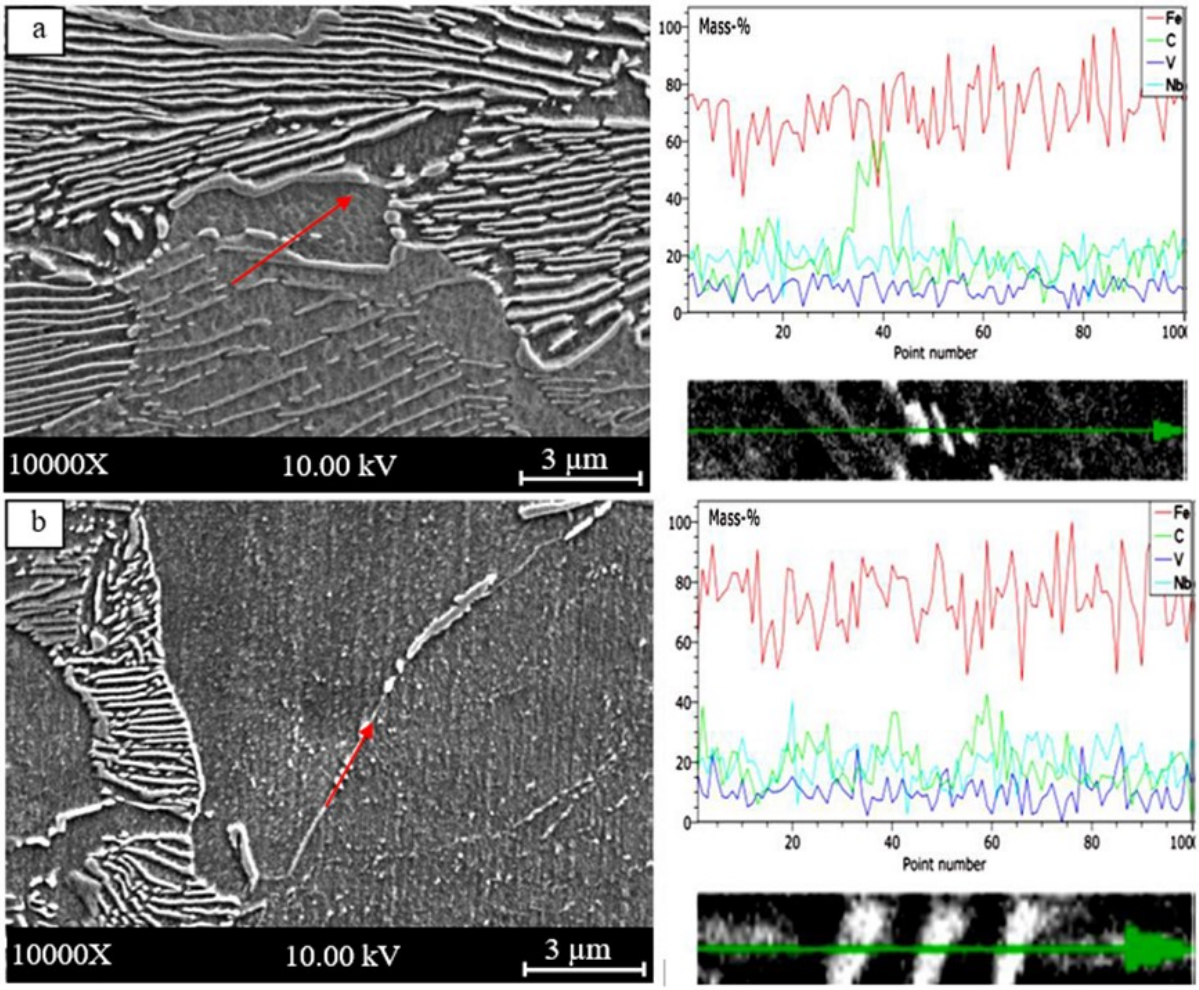

Figure 7. Line EDS analysis obtained from the (a) homogenised and (b) 20% deformed samples.

Stress-strain diagrams and compression test results of sintered, homogenized, 20%, 40% and 60% deformed samples are given in Figure 8 and Table 3 respectively. As is seen, the yield strength (Rp0,2) values of the sintered and homogenised samples are 232 MPa and 282 MPa respectively. An increase in Rp0,2 value is observed with the homogenisation heat treatment. A continuous increase in Rp0.2 values to 322 MPa, 335 MPa and 356 MPa was also observed as the deformation rate increased to 20%, 40% and 60% respectively. Table 3 indicated that the hardness results showed a similar behaviour to those of the yield strength results. The hardness values of the sintered and homogenized samples were measured as 100 $Hv_{0,5}$ and 126 $Hv_{0,5}$ respectively. As in the yield strength results, an increase in the hardness value is observed with the homogenization heat treatment which refined the microstructure by decreasing the grain sizes due to higher cooling rates compared to the sintered samples. Hardness of the 20%, 40% and 60% deformed samples continued to increase to 171 $Hv_{0,5}$, 188 $Hv_{0,5}$ and 214 $Hv_{0,5}$ respectively. The grain refinement, precipitation hardening, an increase in density and a decrease in porosity of the deformed samples raised the hardness as in the yield strength.

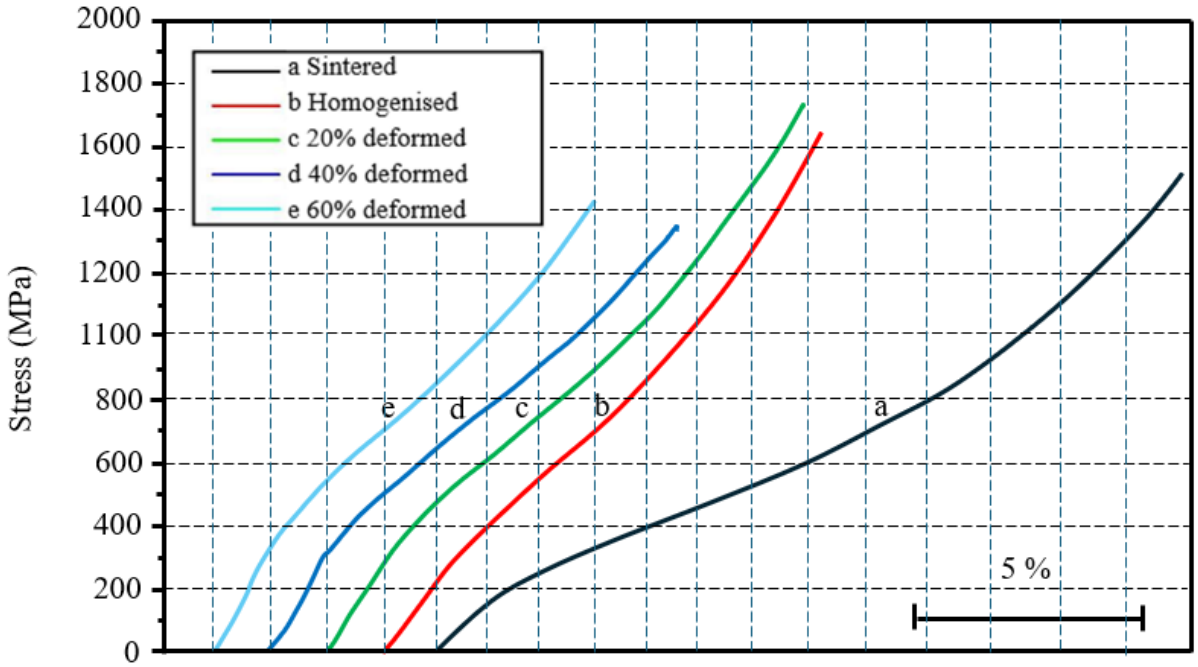

Figure 8. Stress and strain diagrams of sintered, homogenised, 20%, 40% and 60% deformed samples.

Table 3. Yield strength and hardness results of sintered, homogenised, 20%, 40% and 60% deformed PM microalloyed steel.

PM steel	Rp0,2 (MPa) ± σ (SD)	Hv0,5±σ (SD)
Sintered	232±4,64	100± 2,11
Homogenised	282±5,64	126±2,52
20% deformed	322±6,44	171±3,42
40% deformed	335±6,71	188±3,76
60% deformed	356±7,12	214±4,28

Compression and hardness test results indicated that the yield strength and hardness increased when the microalloyed PM steel was homogenized or deformed in the range of 20%, 40% and 60%. The reason for this is that the occurrence of grain refinement and precipitate strengthening affected both yield strength and hardness. Interphase precipitation during the γ/α transformation generally contributes to the strength increment in thermomechanically deformed microalloyed steels. Moreover, significant precipitation hardening of steel can be achieved even if the amount of precipitate is at a low volume fraction [35]. Nb, V and Ti, which form carbides and nitrides, are added to the steel in single or multiple combinations, increase the strength through grain refinement and precipitation hardening. In this way, the mechanical properties of microalloyed steel are increased [36].

It is known that the addition of Nb to low alloy steels provides higher yield strengths. Similar to the strength increment with grain refinement, fine Nb(C,N) precipitates play an important role to increase the strength by preventing dislocation and grain boundary movement. Nb can form as Nb(C,N) in steel and the volume fraction and sizes of Nb(C,N) have a significant

effect on the precipitate hardening. The higher volume fraction and the finer precipitate sizes of Nb(C,N) increases precipitate hardening effect significantly. During the phase transformation Nb atoms combine with C or N atoms at the austenite/ferrite interface to form Nb(CN). With the decrease in austenite/ferrite transformation temperature, the driving force required for the formation of Nb(CN) increases [37]. Funakawa et al. [38] showed that interphase precipitation could increase the strength about 300 MPa according to theoretical calculation. For Nb-steel, where the solubility difference between nitride and carbide is relatively small, mixed carbonitrides form at all nitrogen contents, even at high stoichiometric levels. Nb(C,N) is stable at low temperatures of austenite but dissolves at higher temperatures, which subsequently causes deformation-induced precipitation. The deformed austenite structure transforms to fine-grained ferrite during cooling and provides high mechanical properties. The increased precipitation of the solute Nb in smaller sizes within the ferrite additionally causes an increase in strength [39].

The dissolution temperature of Nb is higher than the V. Nb can coexist with V at lower reheating temperatures. In this case, Nb has an effect on grain refinement, while V has a higher effect on precipitation hardening. In addition, since the dissolution temperature of V is low, grain coarsening may occur in deformed steel at high temperatures. The addition of V and Nb can refine the grains, delay the recrystallization of austenite, and retard the γ/α transformation, regardless of the manner in which the two elements in the austenite phase dissolve or precipitate [36]. In the present work, the solubility product of NbC and VC at 1150°C was calculated by using equation (1) and (2) given by Narita [40]. The solubility product of VC and NbC was found to be 1,1 and $7{,}38\times10^{-3}$, respectively. It is clear that the solubility of VC is higher than NbC, and therefore V and C atoms should be present in the solution during sintering at 1150 °C. This soluble V will precipitate as VC in austenite or ferrite depending on cooling rate after sintering, homogenisation or deformation. Precipitate formation in microalloyed steels can occur during the γ/α phase transformation because the driving force for the precipitation of microalloyed carbonitrides increases during the γ/α transformation. Additionally, due to the different solubility of carbonitrides in the two phases, a high amount of precipitation can occur in ferrite. The solubility of VC in austenite is considerably higher those of the other microalloy carbides and nitrides, suggesting that VC will be completely dissolved even at low austenitising temperatures (900°C) given that the V level is typical of that used in microalloyed steels (up to 0.15wt.% in the case of V). Therefore these V and C in solution are more effective in the precipitation hardening mechanism by precipitating during cooling [2,41]. An increase in strength of microalloyed PM steels is due to precipitation hardening, resulting in the formation of NbC and VC.

$\log [Nb\%]_\gamma [C\%]_\gamma = - 7900 / T + 3.42$ ..... (1)
$\log [V\%]_\gamma [C\%]_\gamma = - 9500 / T + 6.72$ ..... (2)

In the present experimental work, the amount of Nb as NbC can also be obtained from the steel composition, solubility product data given in equation (1) and from equation (3), the weight percentage of NbC can be obtained simply by substitution of NbC in equation (4) [2].

$$Nb_{NbC} = \frac{A_{Nb}[((C_T + Nb_T A_C)/A_{Nb}) - (((C_T + Nb_T A_C/A_{Nb})^2 - (4A_C(Nb_T C_T - k_s)/A_{Nb}))^{1/2}]}{2A_C} \quad \text{.....(3)}$$

$$(NbC) = \frac{Nb_{NbC}\,(A_{Nb} + A_C)}{A_{Nb}} \quad \text{.....(4)}$$

From these equations the amount of NbC at 1150ºC were found to be 0.085 wt.%. An analyses of the equilibrium precipitation of MX-type phases indicated that NbC has higher thermal stability than VC. Thus, the amount of NbC which is undissolved at a given temperature and is available for grain growth inhibitation and dissolved V and C content that are available for the formation of fine interphase precipitation during cooling. NbC precipitates restrict grain growth during sintering, homogenisation or hot deformation and the finer austenite grain size increases the strength of the steel containing Nb. V microaddition does not affect the formation of fine-grained austenite microstructure through VC dispersive particles but it can enhance the strength of the steel by its hardenability effect [2,42].

When the mechanical properties of sintered, homogenised, 20%, 40% and 60% deformed microalloyed PM steels were compared with eachother, the highest yield strength and hardness values were obtained in the 60% deformed samples, and followed by 40% deformed, 20% deformed, homogenised and sintered samples. Higher amount of deformation at the austenite increased nucleation sites such as annealing twins and deformation bands which are favourable sides for phase transformation [19,28,43]. This provides the formation of a finer structure, causing the precipitates to be dispersed homogeneously. As a result, mechanical properties increase. As it is also known, density is one of the important factors affecting the mechanical properties of PM steels. If the density is high, mechanical properties of PM steel increase, because volume fraction of pores decreases with increasing the density. Pores in steel causes the stresses accumulation which contribute to crack propagation [44,45].

4. Conclusion

In this study, Nb-V microalloyed PM steel was produced and deformed at 1150-930°C to control density and precipitate formation simultaneously. The aim of this study is to investigate the relationship between microstructure and mechanical properties of PM microalloyed steel under sintered, homogenised, 20%, 40% and 60% deformed conditions. The general results obtained from present work are listed as follows:

1. The microalloyed PM steel consists of ferrite, pearlite and a porous structure under sintered, homogenised, 20%, 40% and 60% deformed conditions. The density of the sintered and homogenized samples increased with increasing deformation rate. Also finer ferrite and pearlite phase distributed more homogenuously were observed with increasing deformation rate.

2. The homogenised samples have smaller grains than the sintered samples. This is due to the fact that homogenised samples were cooled faster than sintered samples. At higher cooling rates such as air cooling, grain refinement occurs before the austenite-ferrite transformation. Also, the grain sizes decreased when the deformation rate increased. Strain induced precipitates such as NbC or VC occurred during deformation and prevented grain growth resulted in finer structure.

3. Ferrite volume fraction of homogenised and deformed samples increased compared to the sintered samples. This is due to smaller grain sizes in homogenised and deformed samples which accelerated nucleation rate of ferrite by rising the amount of strained region at the austenite grain and grain boundaries.

4. An increase in yield strength and hardness of microalloyed PM steel is observed with the homogenisation heat treatment. A continuous increase in yield strength and hardness was also

observed as the deformation rate increased. The reason for this is that the occurrence of grain refinement and precipitate strengthening affect both yield strength and hardness of microallyed PM steel under different conditions.

5. Thermomechanical process, applied to the microalloyed PM steel, can improve the mechanical properties by increasing density, grain refinement and precipitation strengthening without raising the alloying element additions.

Acknowledgments

This work was supported by Scientific Research Projects Coordination Unit of Karabük University. Project Number: FDK-2020-2318.

Author's contributions

D. Taştemür: Conceptualization, Methodology, Investigation, Data analysis, writing – original draft. S. Gündüz: Investigation, Data analysis, Discussion, Writing – original draft.

Data Availability

The data that support the findings of this study are available from the corresponding author, Süleyman Gündüz, upon reasonable request.

Conflict of interest

On behalf of all authors, the corresponding author states that there is no conflict of interest.

References

1. C. Schade, T. Murphy, A. Lawley, R. Doherty, Microstructure and mechanical properties of microalloyed PM steels, International Journal of Powder Metallurgy, 48 (6) (2012) 51-59. https://www.researchgate.net/publication/267383935

2. T. Gladman, The physical metallurgy of microalloyed steels, The Institute of Materials, London, 1997, p.105-110.

3. F. Bakkali El Hassania, A. Chenaouia, R. Dkiouaka, L. Elbakkalib, A. Al Omarc, Characterization of deformation stability of medium carbon microalloyed steel during hot forging using phenomenological and continuum criteria, Journal of Materials Processing Technology, 1999 (2008) 140–149. https://doi.org/10.1016/j.jmatprotec.2007.08.004

4. M. Akif Erden, S. Gündüz, M. Türkmen, H. Karabulut, Microstructural characterization and mechanical properties of microalloyed powder metallurgy steels, Materials Science and Engineering A, 616 (2014) 201–206. https://doi.org/10.1016/j.msea.2014.08.026

5. T. Gladman, Grain refinement in multiple microalloyed steels, in: HSLA Steels: Processing, Properties and Applications, Minerals, Metals and Materials Society Warrendale, PA, 1992, 123–125.

6. T. N. Baker, Process, microstructure and properties of vanadium microalloyed steels, Materials Science and Technology, 25 (9) (2009) 1083–1107.

https://doi.org/10.1179/174328409X453253

7. S. Gündüz, M. A. Erden, H. Karabulut, M. Türkmen, The Effect of vanadium and titanium on mechanical properties of microalloyed PM steel, Powder Metallurgy and Metal Ceramics, 55 (5-6) (2016) 277-287. https://doi.org/1068-1302/16/0506-0277

8. W. B. Morrison, Microalloy steel-the beginning, Materials Science and Technology, 25 (9) (2009) 1066-1073. https://doi.org/10.1179/174328409X453299

9. M. Opiela, Effect of thermomechanical processing on the microstructure and mechanical properties of Nb-Ti-V Microalloyed, Journal of Materials Engineering and Performance, 23 (2014) 3379-3388. https://doi.org/10.1007/s11665-014-1111-8

10. E. Eghbali, A. Abdollah-zadeh, Influence of deformation temperature on the ferrite grain refinement in a low carbon Nb-Ti microalloyed steel, Journal of Materials Processing Technology, 180 (2006) 44–48. https://doi.org/10.1016/j.jmatprotec.2006.04.018

11. S. L. Grajcar, Effect of Nb microaddition on a microstructure of low- alloyed steels with increased manganese content, Materials Science Forum, 706 (2012) 2124–2129. https://doi.org/10.4028/www.scientific.net/MSF.706-709.2124

12. M. Gomez, S. F. Medina, A. Quispe, P. Valles, Static recrystallization and induced precipitation in a low Nb microalloyed SteeI, Iron and Steel Institute of Japon International, 42 (4) (2002) 423–431. https://doi.org/10.2355/isijinternational.42.423

13. M. Akif Erden, S. Gündüz, H. Karabulut, M. Türkmen, Effect of vanadium addition on the microstructure and mechanical properties of low carbon microalloyed powder metallurgy steels, Materials Testing, 58 (5) (2016) 433-437. https://doi.org/10.3139/120.110875

14. C. Schade, T. Murphy, A. Lawly, R. Doherty: Microstructure and mechanical properties of PM steels alloyed with silicon and vanadium, International Journal of Powder Metallurg, 48 (2012) 41-48. https://www.researchgate.net/publication/267425992_

15. A. Ghosh, S. Das, S. Chatterjee, B. Mishra, P. Ramachandra Rao, Influence of thermo-mechanical processing and different post-cooling techniques on structure and properties of an ultra low carbon Cu bearing HSLA forging, Materials Science and Engineering A, 348 (1–2) (2003) 299–308. https://doi.org/10.1016/S0921-5093(02)00735-9

16. Y. Babayev, Optimization of production of a compressor body by using methods of powder metallurgy and diffusion welding, Ph.D thesis, Dokuz Eylül University Institute of Science and Technology, 2007.

17. A. Ayata, Investigation of sinterability of powder metal aluminum materials with microwave energy, M.Sc thesis, Gazi University Institute of Science and Technology, 2007.

18. D. Taştemür, S. Gündüz, M. A. Erden, Investigation of thermomechanical processing of Nb microalloyed steel produced by powder metallurgy, Gazi University Journal of Science, 35 (2) (2022) 606-616. https://doi.org/10.35378/gujs.835371

19. A. G. Yirik, S. Gündüz, D. Taştemür, M.A. Erden, Microstructural and mechanical properties of hot deformed AISI 4340 steel produced by powder metallurgy, Science of Sintering, 55 (2023) 45-56. https://doi.org/10.2298/SOS2301045Y

20. J. G. Jung, J. S. Park, J. Kim, Y. K. Lee, Carbide precipitation kinetics in austenite of a Nb–Ti–V microalloyed steel, Materials Science and Engineering A, 528 (16-17) (2011) 5529-5535. https://doi.org/10.1016/j.msea.2011.03.086

21. D. Hernandez, B. López, J. M. Rodriguez-Ibabe, Ferrite grain size refinement in vanadium microalloyed structural steels, Materials Science Forum, 500 (2005) 411-418. https://doi.org/10.4028/www.scientific.net/MSF.500-501

22. R. D. K. Misra, K. K. Tenneti, G. C. Weatherly, G. Tither, Microstructure and texture of hot-rolled Cb-Ti and V-Cb microalloyed steels with differences in formability and toughness, Metallurgical and Materials Transactions A, 34 (2003) 2341-2351. https://doi.org/10.1007/s11661-003-0297-4

23. P. C. M. Rodrigues, E. V. Pereloma, D. B. Santos, Mechanical properities of an HSLA bainitic steel subjected to controlled rolling with accelerated cooling, Materials Science and Engineering A, 283 (1-2) (2000) 136-143. https://doi.org/10.1016/S0921-5093(99)00795-9

24. M.A. Erden, An investigation on the relationship between microstructure and mechanical properties of microalloyed steels produced by powder metallurgy, Ph.D thesis, Karabük University Institute of Science and Technology, 2015.

25. H. Karabulut, M. Türkmen, M. A. Erden, S. Gündüz, Effect of different current values on microstructure and mechanical properties of microalloyed steels joined by the submerged arc welding method, Metals, 6 (11) (2016) 2-7. https://doi.org/10.3390/met6110281

26. M.A. Erden, The effect of the sintering temperature and addition of niobium and vanadium on the microstructure and mechanical properties of microalloyed PM steels. Metals, 7 (9) (2017) 2-16. https://doi.org/10.3390/met7090329

27. M.A. Erden, The effect of sintering time on tensile strength of Nb-V microalloyed powder metallurgy steels, Technological and Applied Sciences, 15 (1) (2020) 15–22. https://doi.org/10.12739/NWSA.2020.15.1.2A0180

28. I. Tamura, C. Ouchi, T. Tanaka, H. Sekine, Thermomechanical processing of high-strength low-alloy steels, Butterworths, Cornwall, 1988, p. 100.

29. R.C. Cochrane, in Phase Transformations in Steels (Eds. E. Pereloma, D.V. Edmonds, Woodhead Publishing, Cambridge, 2012, p. 153–212.

30. A. Pandit, A. Murugaiyan, A. S. Podder, A. Haldar, D. Bhattacharjee, S. Chandra, R. K. Ray, Strain induced precipitation of complex carbonitrides in Nb–V and Ti–V microalloyed steels, Scripta Materialia, 53 (11) (2005) 1309-1314. https://doi.org/10.1016/j.scriptamat.2005.07.003

31. M. Tenerowicz, M. Sułowski, The effect of Mn content on the structure and properties of PM Mn steels, Archives of Metallurgy and Materials, 62 (4) (2017) 2153-2163.

https://doi.org/10.1515/amm-2017-0318

32. M.G. Akben, T. Chandra, P. Plassiard, J.J. Jonas, Dynamic precipitation and solute hardening in a titanium microalloyed steel containing three levels of manganese, Acta Metallurgica, 32 (1984) 591–601. https://doi.org/10.1016/0001-6160(84)90070-1

33. Z. Wanga, X. Sun, Z. Yang, Q. Yong, C. Zhang, Z. Li, Y. Weng, Effect of Mn concentration on the kinetics of strain induced precipitation in Ti microalloyed steels, Materials Science & Engineering A, 561 (2013) 212–219.
https://doi.org/10.1016/j.msea.2012.10.085

34. A. Grajcar, W. Zalecki, W. Burian, A Kozłowska, Phase equilibrium and austenite decomposition in advanced high-strength medium-Mn bainitic steels, Metals 6 (2016) 248-261. https://doi.org/doi:10.3390/met6100248

35. F. Z. Bu, X. M. Wang, S. W. Yang, C. J. Shang, R. D. K. Misra, Contribution of interphase precipitation on yield strength in thermomechanically simulated Ti–Nb and Ti–Nb–Mo microalloyed steels, Materials Science and Engineering A, 620 (2015) 22-29.
https://doi.org/10.1016/j.msea.2014.09.111

36. X. Li, J. Zhao, J. C. Bao, B. Q. Ning, J. P. Li, Microstructure transformation of Nb-V microalloyed steel during continuous cooling process, Advanced Materials Research, 590 (2012) 23-27. https://doi.org/10.4028/www.scientific.net/AMR.590

37. L. Y. Sun, X. Liu, X. Xu, S. W. Lei, H. G. Li, Q. J. Zhai, Review on niobium application in microalloyed steel, Journal of Iron and Steel Research International, 29 (10) (2022) 1513-1525. https://doi.org/10.1007/s42243-022-00789-1

38. Y. Funakawa, T. Shiozaki, K. Tomita, T. Yamamoto, E. Maeda, Development of high strength hot-rolled sheet steel consisting of ferrite and nanometer-sized carbides, Iron and Steel Institute of Japon International, 44 (11) (2004) 1945-1951. https://doi.org/10.2355/isijinternational.44.1945

39. Y. L. Wang, L. C. Zhuo, M. W. Chen, Z. D. Wang, Thermodynamic model for precipitation of carbonitrides in microalloyed steels and its application in Ti–V–C–N system, Rare Metals, 35 (2016) 735-741. https://doi.org/10.1007/s12598-015-0495-4

40. K. Narita, Physical chemistry of the groups IVa (Ti, Zr), Va (V, Nb, Ta) and the rare earth elements in steel, Transactions of the Iron and Steel Institute of Japan, 15 (1975) 145-152.
https://doi.org/10.2355/ISIJINTERNATIONAL1966.15.145

41. R. Lagneborg, B. Hutchinson, T. Siwecki, S. Zajac, The role of vanadium in microalloyed steels, Swerea KIMAB, Sweden, 2014, p. 31.

42. M. Opielan, A. Grajcar, Elaboration of forging conditions on the basis of the precipitation analysis of MX-type phases in microalloyed steels, Archives of Civil and Mechanical Engineering, 12 (2012) 427–435.

43. E.U. Morales-Cruz, M. Vargas-Ramírez, A. Lobo-Guerrero, A. Cruz-Ramírez, E. Colin-García, R.G. Sánchez-Alvarado, V.H. Gutiérrez-Pérez, J.M. Martínez-Vázquez, Effect of low

aluminum additions in the microstructure and mechanical properties of hot forged high-manganese steel, Journal of Mining and Metallurgy, Section B: Metallurgy, 59 (1) (2023) 77-90. https://doi.org/10.2298/JMMB220919007M.

44. S. Qing-yun, L. Gui-yan, Q. Li-feng, Y. Ping-yuan, Effect of cooling rate and coiling temperature on precipitate in ferrite of a Nb-V-Ti microalloyed strip steel, Journal of Iron and Steel Research, 14 (5) (2007) 316-319. https://doi.org/10.1016/S1006-706X(08)60102-8

45. D. Wilbert, W. Ángel, L. T. Jurado, J. C. Alcalá, E. C. Martínez, V. V. Cedeño, Effect of copper on the mechanical properties of alloys formed by powder metallurgy, Material Design, 58 (2012) 12–18. https://doi.org/10.1016/j.matdes.2014.02.002

Table captions in this article:

Table 1. Spectral analysis results of sintered Fe-0.35C-0.1Nb-0.1V (wt.%) steel.

Table 2. Density (%), pores (%), ferrite (%), pearlite (%) and grain size values of PM microalloyed steel.

Table 3. Yield strength and hardness results of sintered, homogenised, 20%, 40% and 60% deformed PM microalloyed steel.

Figure captions in this article:

Figure 1. SEM images of (a) Fe, (b) Graphite, (c) Nb and (d) Ti powders.

Figure 2. Schematic presentation of sintering process.

Figure 3. Process steps used in the experimental study.

Figure 4. Produced samples a) sintered, b) homogenized, c) 20%, d) 40% and e) 60% deformed.

Figure 5. OM and SEM microstructure of the PM microalloyed steel at different magnifications; (a,b) sintered and (c,d) homogenised samples.

Figure 6. OM and SEM microstructure of the PM microalloyed steel at different magnifications; (a,b) 20%, (c,d) 40% and (e,f) 60% deformed samples.

Figure 7. Line EDS analysis obtained from the (a) homogenised and (b) 20% deformed samples.

Figure 8. Stress and strain diagrams of sintered, homogenised, 20%, 40% and 60% deformed samples.